ACS NANO
Cite This: ACS Nano 2019, 13, 9664–9672
www.acsnano.org

ARTICLE

High-Modulus Hexagonal Boron Nitride Nanoplatelet Gel Electrolytes for Solid-State Rechargeable Lithium-Ion Batteries

Woo Jin Hyun,[†] Ana C. M. de Moraes,[†] Jin-Myoung Lim,[†] Julia R. Downing,[†] Kyu-Young Park,[†] Mark Tian Zhi Tan,[†] and Mark C. Hersam*[,†,‡,#,§]

[†]Department of Materials Science and Engineering, [‡]Department of Chemistry, [#]Department of Medicine, and [§]Department of Electrical Engineering and Computer Science, Northwestern University, Evanston, Illinois 60208, United States

Supporting Information

ABSTRACT: **Solid-state electrolytes based on ionic liquids and a gelling matrix are promising for rechargeable lithium-ion batteries due to their safety under diverse operating conditions, favorable electrochemical and thermal properties, and wide processing compatibility. However, gel electrolytes also suffer from low mechanical moduli, which imply poor structural integrity and thus an enhanced probability of electrical shorting, particularly under conditions that are favorable for lithium dendrite growth. Here, we realize high-modulus, ion-conductive gel electrolytes based on imidazolium ionic liquids and exfoliated hexagonal boron nitride (hBN) nanoplatelets. Compared to conventional bulk hBN microparticles, exfoliated hBN nanoplatelets improve the mechanical properties of gel electrolytes by 2 orders of magnitude (shear storage modulus ~5 MPa), while retaining high ionic conductivity at room temperature (>1 mS cm^{-1}). Moreover, exfoliated hBN nanoplatelets are compatible with high-voltage cathodes (>5 V *vs* Li/Li$^+$) and impart exceptional thermal stability that allows high-rate operation of solid-state rechargeable lithium-ion batteries at temperatures up to 175 °C.**

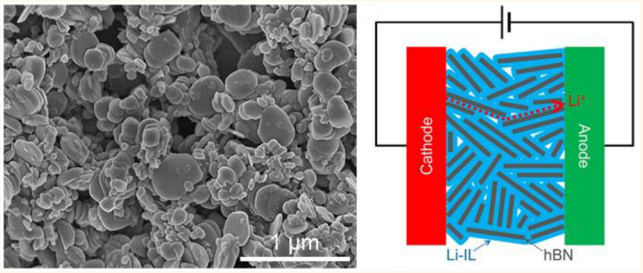

KEYWORDS: *hexagonal boron nitride, ionic liquid, gel electrolyte, lithium-ion battery, mechanical modulus, electrochemical stability, thermal stability*

Lithium-ion batteries are the primary power source for portable electronics and electric vehicles, as well as a core element of grid-level energy management systems. Their deployment in an increasing range of applications has motivated substantial efforts to advance rechargeable lithium-ion battery technology.[1−5] Electrolytes are an essential component of lithium-ion batteries by enabling the reversible transport of lithium ions between the anode and cathode. Typical lithium-ion battery electrolytes are based on lithium salts and organic solvents, which require a porous membrane to physically separate the electrodes and prevent electrical shorting. In addition, liquid electrolytes based on organic solvents are highly flammable, which compromises safety and can lead to catastrophic battery failure. These stability concerns associated with conventional liquid electrolytes have become even more acute as lithium-ion batteries advance toward higher energy densities.[6,7] Consequently, increasing attention has been devoted to the development of solid-state electrolytes that eliminate flammable organic solvents from lithium-ion batteries.[8−11] However, currently available solid-state electrolytes present other significant challenges including low ionic conductivity, high interfacial resistance, and cumbersome processing, which has impeded their utilization in most lithium-ion battery contexts.

Electrolytes based on ionic liquids and a gelling matrix, also referred to as ion gels or ionogels, are promising candidates for solid-state lithium-ion batteries.[12,13] Compared to the organic solvents used in traditional liquid electrolytes, ionic liquids offer several advantages including nonflammability, negligible vapor pressure, and high thermal and electrochemical stability.[14−16] Moreover, when combined with a gelling matrix, ionic liquids form a composite solid-state electrolyte that can replace both the liquid electrolyte and separator in a single component. This consolidation of multiple functionalities into a single component allows for simplified packaging, streamlined manufacturing, and minimal risk of leakage. Furthermore, the mechanical strength enhancement from the gelling matrix provides improved resistance to lithium dendrite growth in

Received: June 25, 2019
Accepted: July 18, 2019
Published: July 18, 2019

DOI: 10.1021/acsnano.9b04989
ACS Nano 2019, 13, 9664–9672

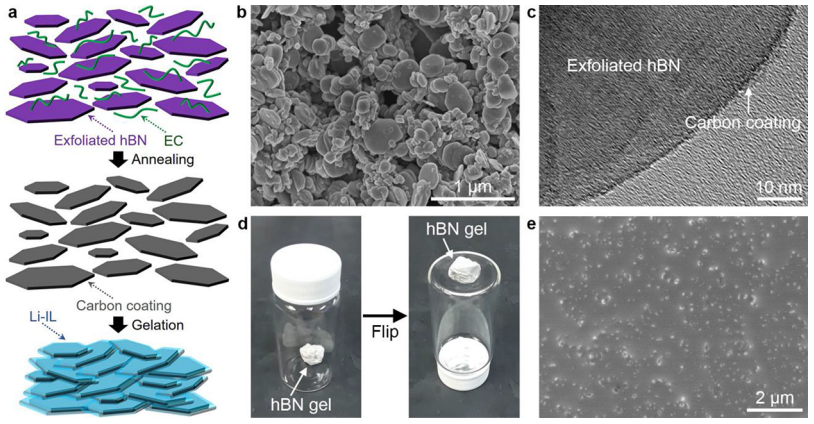

Figure 1. Hexagonal boron nitride (hBN) nanoplatelets and gel electrolytes. (a) Schematic diagram of hBN gel electrolyte preparation. hBN nanoplatelets are exfoliated from bulk hBN microparticles by a liquid-phase exfoliation method with ethyl cellulose (EC) stabilizers. The resulting exfoliated hBN/EC powder is annealed to decompose EC at 400 °C for 2 h, which generates a thin carbon coating on the surface of the hBN nanoplatelets. Finally, the hBN nanoplatelets and a lithium ionic liquid (Li-IL) are mixed to formulate gel electrolytes. (b) Scanning electron microscopy (SEM) image of the exfoliated, carbon-coated hBN nanoplatelets. (c) Transmission electron microscopy (TEM) image of the exfoliated, carbon-coated hBN nanoplatelets. The dark band (indicated by the arrow) at the edge of the exfoliated hBN nanoplatelet corresponds to the carbon coating. (d) Photographs of a vial with the hBN gel electrolyte before (left) and after (right) flipping. The electrolyte does not move from the bottom of the inverted vial, confirming the formation of a stable gel. (e) SEM image of the hBN gel electrolyte.

lithium metal batteries.[17−19] While these desirable mechanical properties can be enhanced by increasing the solid matrix loading,[19−21] this approach leads to a trade-off with ionic conductivity since increased solid loading impedes ion motion. Hence, despite extensive research into ionic liquid gel electrolytes based on diverse polymer and ceramic particle matrices,[19−25] mechanical properties have typically been compromised to impart high ionic conductivity.

Here, we report the development of high-modulus, ion-conductive gel electrolytes using imidazolium ionic liquids and exfoliated hexagonal boron nitride (hBN) nanoplatelets. As a solid matrix material, hBN possesses several desirable attributes including electrically insulating character, chemical inertness, thermal stability, and mechanical robustness.[26−28] However, the difficulty in controlling the size of conventional bulk hBN microparticles hampers strong solidification of ionic liquid gels, resulting in poor mechanical strength.[29] Using a scalable liquid-phase exfoliation method, we produce homogeneous hBN nanoplatelets that adsorb large quantities of ionic liquids, leading to significant enhancement of the mechanical modulus of gel electrolytes by 2 orders of magnitude, while maintaining high ionic conductivity. Moreover, the hBN nanoplatelet solid matrix improves electrochemical stability at high potentials, which enables compatibility with high-voltage cathodes such as lithium nickel manganese oxide. Finally, the high thermal stability of the hBN nanoplatelet solid matrix facilitates high-rate operation of solid-state rechargeable lithium-ion batteries at temperatures up to 175 °C.

RESULTS AND DISCUSSION

Exfoliation of hBN and Gel Electrolyte Preparation. Figure 1a depicts a schematic of the preparation of ionic liquid gel electrolytes with exfoliated hBN nanoplatelets. The hBN nanoplatelets (Figure 1b) are isolated from bulk hBN microparticles by shear mixing with ethyl cellulose (EC) in ethanol. EC is included in the hBN/ethanol dispersion to stabilize the exfoliated hBN nanoplatelets during shear mixing and thereby improve the yield of liquid-phase exfoliation.[30] The exfoliated hBN nanoplatelets and EC are subsequently collected from the shear-mixed dispersion by flocculation and centrifugation, followed by annealing at 400 °C for 2 h to decompose the EC polymer. This annealing process volatilizes most of the EC, but also leaves behind a thin amorphous carbon coating on the surface of the exfoliated hBN nanoplatelets, as shown by the dark band at the edge of the hBN nanoplatelet in the transmission electron microscopy (TEM) images of Figures 1c and S1 (Supporting Information). This dark band is not observed in TEM images of hBN nanoplatelets exfoliated without EC (Figure S2, Supporting Information). Additionally, due to the amorphous carbon coating, the white hBN nanoplatelet powder (Figure S3, Supporting Information) appears visibly gray after annealing, with X-ray photoelectron spectroscopy (XPS, Figure S4, Supporting Information) confirming the presence of carbon on the hBN nanoplatelet surfaces. Importantly, the hBN nanoplatelets retain their electrical insulating properties even after the carbon coating. With a yield of 7%, bulk hBN microparticles (~1 μm particle diameter) are exfoliated into hBN nanoplatelets with average lateral size and thickness of 143 ± 67 nm and 2.4 ± 1.2, respectively, as determined by atomic force microscopy (AFM, Figure S5, Supporting Information).

The hBN gel electrolytes are produced by mixing the exfoliated, carbon-coated hBN nanoplatelets (33−40% by weight) and a lithium ionic liquid (Li-IL), 1-ethyl-3-methylimidazolium bis(trifluoromethylsulfonyl)imide (EMIM-TFSI) containing 1 M lithium bis-(trifluoromethylsulfonyl)imide (LiTFSI) salt. The solidification of the gel electrolytes can be observed by the lack of movement of the electrolytes from the bottom of the vial even after it is flipped over (Figure 1d). Quantitatively, the gel electrolytes exhibit a storage modulus (G') that is higher than its loss modulus (G'') with minimal frequency dependence (Figure S6, Supporting Information), revealing reliable solid-like behavior. Moreover, scanning electron microscopy (SEM, Figure 1e) of the gel electrolyte shows that the hBN nanoplatelets are well-coated with Li-IL.

DOI: 10.1021/acsnano.9b04989
ACS Nano 2019, 13, 9664−9672

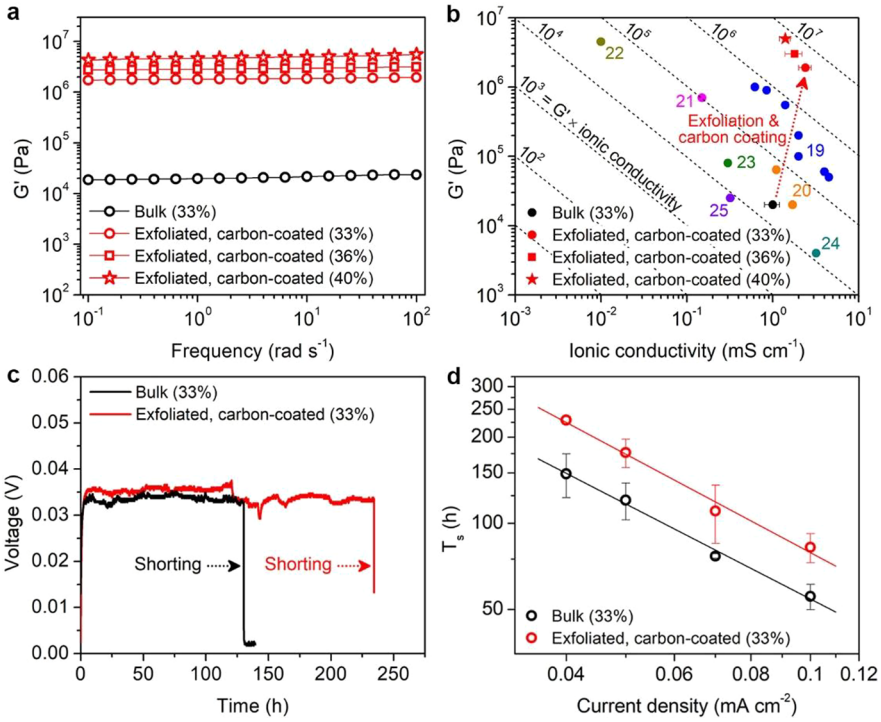

Figure 2. Mechanical modulus, ionic conductivity, and polarization tests. (a) Storage modulus (G') of gel electrolytes using bulk hBN microparticles and exfoliated, carbon-coated hBN nanoplatelets. (b) Comparison to G' and room-temperature ionic conductivity of ionic liquid gel electrolytes previously reported for rechargeable lithium-ion batteries. The dashed lines represent isolines of the product of G' and ionic conductivity, and the number labels refer to the citation numbers in the references. (c) Polarization voltage profiles of lithium symmetric cells (Li|gel electrolyte|Li) with gel electrolytes formulated with bulk hBN microparticles and exfoliated, carbon-coated hBN nanoplatelets, at a current density of 0.04 mA cm^{-2}. The sudden voltage drop indicates the formation of short circuits by lithium dendrites. (d) Short-circuit formation time (T_s) of the lithium symmetric cells as a function of current density. The data points describe the average and standard deviation from three samples.

Mechanical Properties and Ionic Conductivity. To investigate the influence of the exfoliation and carbon coating of hBN on mechanical properties, shear storage moduli (G') of the gel electrolytes formulated using the exfoliated, carbon-coated hBN nanoplatelets and the bulk hBN microparticles are compared, as shown in Figure 2a. The exfoliated, carbon-coated hBN gel electrolyte presents a storage modulus that is 2 orders of magnitude higher than that of the bulk hBN gel electrolyte at the same solid loading. These enhanced mechanical properties can be primarily attributed to the smaller size of the exfoliated hBN nanoplatelets. Since gelation originates from attractive forces between hBN particles, the reduced size of exfoliated hBN nanoplatelets reinforces gelation due to the enlarged surface area for interparticle interactions.[31] Another contribution to the improved mechanical properties arises from the amorphous carbon coating on the hBN surface, which can be identified by comparing gel electrolytes prepared with pristine and carbon-coated bulk hBN microparticles (Figure S7, Supporting Information). This improvement can be attributed to the surface chemistry change following carbon coating, which strengthens the interparticle interactions among the hBN nanoplatelets.[31] Therefore, it is apparent that EC not only improves the liquid-phase exfoliation yield but also enhances the mechanical properties of the gel electrolytes through its amorphous carbon coating following annealing. Importantly, the significant enhancement of the mechanical modulus occurs without compromising ionic conductivity, as shown in Figure 2b. This minimal trade-off between mechanical properties and ionic conductivity can be attributed to the nanoscale size of exfoliated hBN, which leads to stronger gelation without significantly disrupting ionically conductive pathways in the gel electrolytes. Overall, the ionic liquid gel electrolytes based on exfoliated, carbon-coated hBN nanoplatelets possess exceptional mechanical properties (shear storage modulus as high as 5 MPa) with high ionic conductivities at room temperature (>1 mS cm^{-1}) that outperform all other ionic liquid gel electrolytes previously reported for rechargeable lithium-ion batteries,[19−25] as shown in Figure 2b. Furthermore, the compressive elastic modulus of the hBN gel electrolyte (40% hBN) has a high value of 31 MPa, and the lithium-ion transference number is 0.18, which is double that of previously reported gel electrolytes based on piperidinium ionic liquids and bulk hBN.[29] Finally, the interfacial resistance of the hBN gel electrolyte with lithium metal electrodes is 14 Ω cm^2 (Figure S8, Supporting Information), which is 1 order of magnitude lower than that of rigid garnet electrolytes.[32,33]

The large mechanical modulus is also valuable for strengthening the resistance of the gel electrolytes to lithium dendrite growth for lithium metal batteries.[34] To confirm the enhanced suppression of lithium dendrite growth, galvanostatic polarization tests were performed using lithium symmetric cells. In this polarization method,[19,35] a fixed current density is applied to lithium symmetric cells (Li|electrolyte|Li) to induce lithium dendritic growth, and the cell voltage is measured as a function of time until the appearance of a sudden voltage drop that occurs upon electrode shorting. Figure 2c compares the typical voltage profiles for the polarization of lithium

DOI: 10.1021/acsnano.9b04989
ACS Nano 2019, 13, 9664−9672

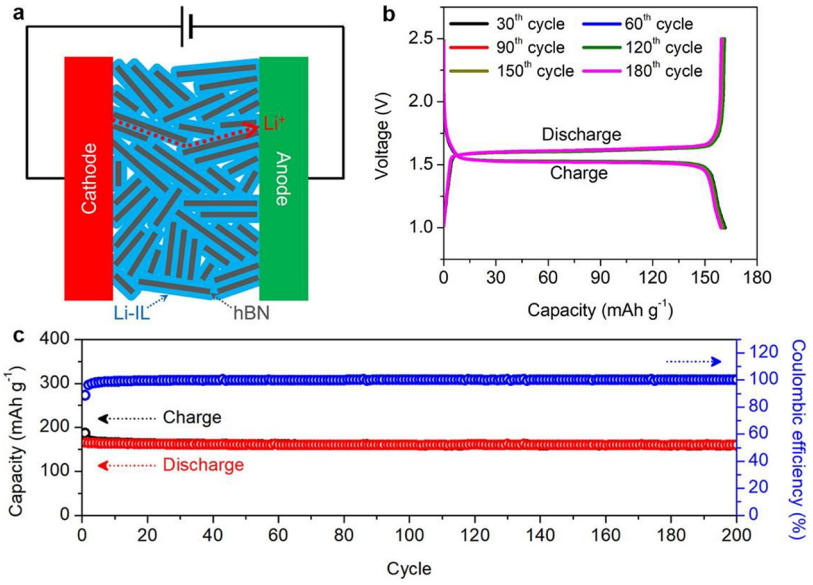

Figure 3. Battery configuration and long-term stability. (a) Schematic of a lithium-ion battery operating with an hBN gel electrolyte. The hBN gel electrolyte separates anode and cathode electrodes without a separator, and lithium ions travel (indicated by the red dotted line) through Li-IL adsorbed on the surface of the hBN nanoplatelets. (b) Charge−discharge voltage profiles of a $Li_4Ti_5O_{12}$ (LTO)|hBN gel|Li cell measured at 0.1C at room temperature, with a voltage window of 1.0−2.5 V. (c) Cycling performance of the cell tested over 200 cycles (>6 months). Black, red, and blue symbols denote gravimetric charge capacity, gravimetric discharge capacity, and Coulombic efficiency, respectively.

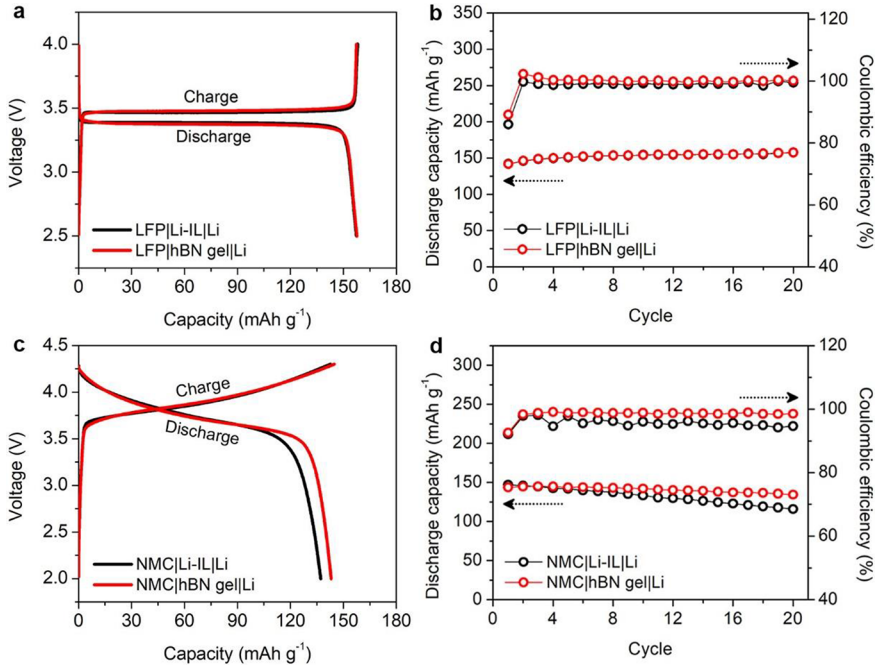

Figure 4. Electrochemical stability for rechargeable lithium-ion batteries. (a) Typical charge−discharge voltage profiles of $LiFePO_4$ (LFP)|hBN gel|Li and LFP|Li-IL|Li cells tested at 0.1C at room temperature, with a voltage window of 2.5−4.0 V. (b) Gravimetric discharge capacity and Coulombic efficiency of the cells. (c) Typical charge−discharge voltage profiles of $LiNi_{0.33}Mn_{0.33}Co_{0.33}O_2$ (NMC)|hBN gel|Li and NMC|Li-IL|Li cells measured at 0.1C at room temperature, with a voltage window of 2.0−4.3 V. (d) Gravimetric discharge capacity and Coulombic efficiency of the cells.

symmetric cells containing gel electrolytes prepared with bulk hBN microparticles and exfoliated, carbon-coated hBN nanoplatelets. At the same current density, the two samples display similar voltage levels, but the exfoliated hBN gel electrolyte exhibits a longer time (T_s) preceding electrode shorting than the bulk hBN gel electrolyte, thus indicating more effective suppression of lithium dendrite growth (Figure S9, Supporting Information). As the current density increases (Figure 2d), T_s decreases due to faster lithium ion movement, but the exfoliated hBN gel electrolyte consistently exhibits longer T_s than the bulk hBN gel electrolyte. Considering their similar ionic conductivities, the longer T_s of the exfoliated hBN gel electrolyte can be attributed to its enhanced mechanical modulus hindering lithium dendrite growth.

DOI: 10.1021/acsnano.9b04989
ACS Nano 2019, 13, 9664−9672

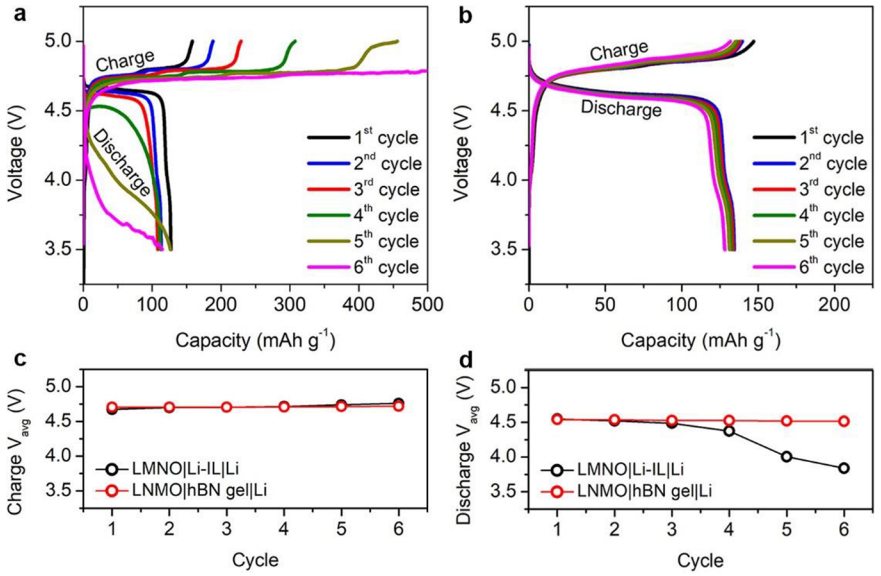

Figure 5. High-voltage lithium-ion batteries. (a) Charge−discharge voltage profiles of a $LiNi_{0.5}Mn_{1.5}O_4$ (LNMO)|Li-IL|Li cell tested at 0.1C at room temperature, with a voltage window of 3.5−5.0 V. (b) Charge−discharge voltage profiles of an LNMO|hBN gel|Li cell measured with the same conditions. (c) Average voltage (V_{avg}) of the charge curves of the cells as a function of cycle. (d) V_{avg} of the discharge curves of the cells as a function of cycle.

To further investigate the influence of the mechanical modulus, lithium plating/stripping tests were performed using lithium symmetric cells with the bulk and exfoliated, carbon-coated hBN gel electrolytes. During the initial cycles (Figure S10a, Supporting Information), the electrolytes exhibit similar voltage profiles, but the bulk hBN gel electrolyte shows a significant increase in the overpotential after 180 cycles (Figure S10b, Supporting Information). This overpotential increase is due to inhomogeneous lithium deposition and severe electrolyte decomposition, leading to thickening solid-electrolyte-interphase (SEI) layers.[36] In contrast, the exfoliated, carbon-coated hBN gel electrolyte presents favorable lithium plating/stripping behavior over 275 cycles, verifying more stable lithium electrodeposition as a result of the enhanced mechanical modulus.

Electrochemical Stability for Rechargeable Lithium-Ion Batteries. Figure 3a depicts a schematic of a lithium-ion battery that employs the exfoliated hBN gel electrolyte. The hBN nanoplatelets serve as the solid framework component of the gel electrolyte that enables battery assembly without a separator between the anode and cathode. The Li-IL adsorbed to the surface of the hBN nanoplatelets facilitates lithium-ion transport between the two electrodes for battery operation. Rechargeable lithium-ion batteries based on the exfoliated hBN gel electrolyte (40% hBN nanoplatelets) were first fabricated using lithium titanium oxide ($Li_4Ti_5O_{12}$, LTO) and lithium metal electrodes. Figure 3b,c displays the charge−discharge voltage profiles and cycling performance, respectively, of the LTO|hBN gel|Li cell tested at 0.1C. The voltage profiles show well-defined plateaus, which indicate effective electrochemical operation using the hBN gel electrolyte. Moreover, the cell retains 96% of its initial gravimetric discharge capacity (1st cycle: 165 mAh g^{-1}; 200th cycle: 159 mAh g^{-1}) and possesses a Coulombic efficiency greater than 99% with negligible change in the voltage profiles over 200 cycles (>6 months), revealing the long-term stability of the hBN gel electrolytes for rechargeable lithium-ion batteries.

To further investigate the electrochemical stability of the hBN gel electrolytes, battery cells were tested employing different cathodes paired with a lithium metal anode (cathode|hBN gel|Li). Control cells were also fabricated using bulk Li-IL as an electrolyte (cathode|Li-IL|Li) with a separator to compare the electrochemical performance with and without the hBN nanoplatelets. Figure 4a displays the typical charge−discharge voltage profiles of the battery cells using a lithium iron phosphate ($LiFePO_4$, LFP) cathode at 0.1C. The LFP|hBN gel|Li cell shows desirable voltage profiles and a gravimetric discharge capacity higher than 150 mAh g^{-1} with a Coulombic efficiency greater than 99% after the first few initial cycles (Figure 4b), which is similar to the behavior of the control cell (LFP|Li-IL|Li). The Coulombic efficiency slightly exceeds 100% for the second and third cycles, which can be attributed to some capacity that was charged in the first cycle (89%) being discharged in the following activation cycles. In addition, for lithium nickel manganese cobalt oxide ($LiNi_{0.33}Mn_{0.33}Co_{0.33}O_2$, NMC) cathodes operating at higher voltages (charge cutoff voltages for LFP and NMC are 4.0 and 4.3 V *vs* Li/Li^+, respectively), enhanced electrochemical performance is observed with the hBN gel electrolyte, as shown in Figure 4c,d. The NMC|hBN gel|Li cell possesses a similar initial gravimetric discharge capacity of 144 mAh g^{-1} to the control cell (NMC|Li-IL|Li), but subsequently exhibits higher discharge capacity and Coulombic efficiency after the few initial cycles.

The improved electrochemical performance with the hBN gel electrolyte can likely be attributed to the adsorption of Li-IL on the large surface area of the hBN nanoplatelets, which stabilizes the Li-IL at high voltages. The enhanced electrochemical stability of the hBN gel electrolyte at high voltages is supported by linear sweep voltammetry (LSV) measurements, as shown in Figure S11 (Supporting Information). The LSV curve of the neat Li-IL electrolyte reveals a decomposition peak at 4.3 V (*vs* Li/Li^+), corresponding to the oxidation of EMIM cations,[37] which is consistent with the degradation of the NMC|Li-IL|Li cell. In contrast, the LSV curve of the

DOI: 10.1021/acsnano.9b04989
ACS Nano 2019, 13, 9664−9672

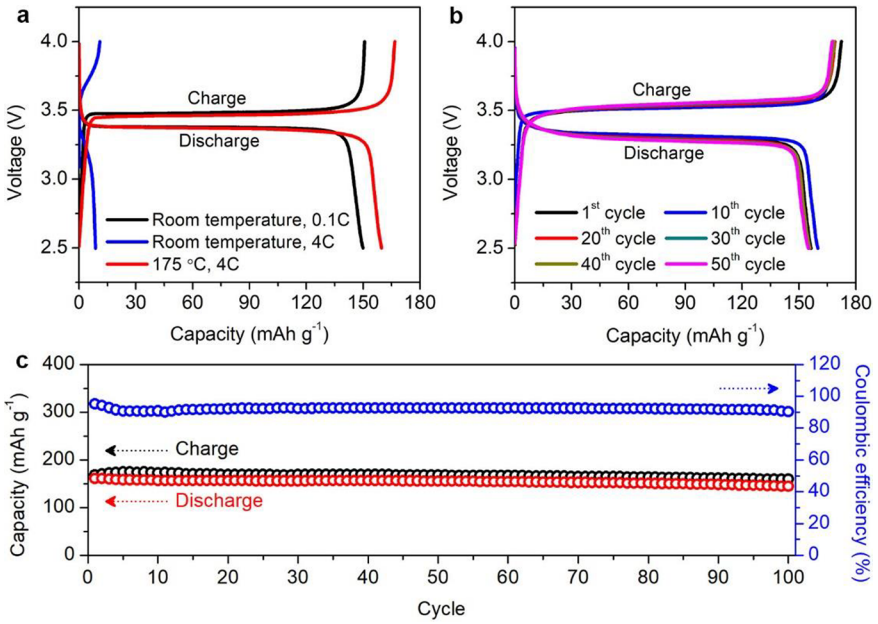

Figure 6. High-temperature battery operation. (a) Typical charge−discharge voltage profiles of a Gr-LFP|hBN gel|Li cell measured at room temperature and 175 °C, with a voltage window of 2.5−4.0 V. The Gr-LFP cathode electrode is composed of LFP active materials and graphene conductive additives. (b) Charge−discharge voltage profiles of the cell at 10C at 175 °C. (c) Cycling performance of the cell tested at 10C at 175 °C. Black, red, and blue symbols denote gravimetric charge capacity, gravimetric discharge capacity, and Coulombic efficiency, respectively.

exfoliated hBN gel electrolyte shows suppression of the decomposition peak and extended electrochemical stability up to 5.3 V (*vs* Li/Li$^+$). In particular, the exfoliated hBN suppresses decomposition more than bulk hBN because of its larger surface area to stabilize Li-IL. The LSV curve suggests that the exfoliated hBN gel electrolyte can be utilized with even higher voltage cathodes. Toward this end, the hBN gel electrolyte was incorporated into cells based on lithium nickel manganese oxide ($LiNi_{0.5}Mn_{1.5}O_4$, LNMO) cathodes operating at a charge cutoff voltage of 5 V (*vs* Li/Li$^+$). While the control cell (LNMO|Li-IL|Li, Figure 5a) shows considerable degradation, the LNMO|hBN gel|Li cell (Figure 5b) exhibits stable operation with an initial gravimetric discharge capacity of 134 mAh g^{-1} and minimal changes in the charge (Figure 5c) and discharge (Figure 5d) voltages upon cycling. It is thus apparent that hBN nanoplatelets enhance the electrochemical stability of ionic liquid gel electrolytes, particularly for high-voltage lithium-ion batteries.

High-Temperature and High-Rate Battery Operation. The thermal stability of the hBN solid matrix and Li-IL implies that hBN gel electrolytes are stable at high temperatures in excess of 300 °C as determined by thermogravimetric analysis (TGA, Figure S12, Supporting Information). When coupled with the nonflammability and negligible vapor pressure of the Li-IL, this thermal stability suggests that hBN gel electrolytes are promising for rechargeable lithium-ion batteries in high-temperature applications such as heat-sterilizable medical devices, thermal reactors, and aerospace technologies. To verify the potential for high-temperature operation, the hBN gel electrolytes were tested using a binder-free cathode, which is composed of LFP active materials and graphene conductive additives (Gr-LFP), and a lithium metal anode. LFP was selected over other cathode materials because of its exceptional structural stability at elevated temperatures.[38,39] In addition, the LFP electrode was prepared without a binder because conventional polyvinylidene fluoride (PVDF) binders limit the battery operating temperature to the melting point of PVDF (~165 °C). Meanwhile, the graphene conductive additive provides high electrical conductivity for favorable charge transport in addition to increased cohesion among the LFP active particles, thereby enabling a mechanically stable electrode film in the absence of a binder (Figure S13, Supporting Information).[40] Furthermore, the high-temperature testing cells were assembled without a separator since the gel electrolyte maintains its solid-state character and thus separates the anode and cathode at elevated temperatures.

Figure 6a shows the charge−discharge voltage profiles of the Gr-LFP|hBN gel|Li cell at room temperature and 175 °C. At room temperature, the cell exhibits a gravimetric discharge capacity of 150 mAh g^{-1} at 0.1C, but the capacity decreases to 9 mAh g^{-1} at 4C. Limited capacity at high C-rates is often observed for solid-state electrolytes due to their relatively low ionic conductances compared to liquid electrolytes. In contrast, when the Gr-LFP|hBN gel|Li cell is operated at 175 °C, the gravimetric discharge capacity increases to 160 mAh g^{-1} at 4C, which originates primarily from the enhanced ionic conductivity of the hBN gel electrolyte at elevated temperatures. As shown in Figure S14 (Supporting Information), the ionic conductivity of the hBN gel electrolyte increases with temperature, in agreement with the Vogel−Fulcher−Tammann model that correlates the ion conduction behavior with free volume and configurational entropy.[41,42] Elevated temperatures also improve lithium diffusion in LFP and charge transfer at the electrolyte/electrode interface, further enhancing high-temperature battery performance.[43−45]

The superlative electrochemical properties of the hBN gel electrolyte at 175 °C allow operation at C-rates up to 10C without decreasing capacity, as shown in Figures 6b and S15 (Supporting Information). Although cycling at 10C shows higher charge and lower discharge voltages than equivalent

DOI: 10.1021/acsnano.9b04989
ACS Nano 2019, 13, 9664−9672

measurements at 4C, the voltage profiles still possess well-defined plateaus and stable operation. Indeed, the cell tested over 100 cycles at 10C at 175 °C (Figure 6c) exhibits a relatively high gravimetric discharge capacity retention of 90% (1st cycle: 160 mAh g^{-1}; 100th cycle: 144 mAh g^{-1}). Stable performance at 175 °C represents the highest reported operating temperature among solid-state rechargeable lithium-ion batteries, confirming the high safety and thermal stability of hBN gel electrolytes for high-temperature applications.

CONCLUSIONS

High-performance solid-state electrolytes have been developed using high-modulus gels based on exfoliated, carbon-coated hBN nanoplatelets and EMIM-TFSI ionic liquid containing LiTFSI salt. Compared to conventional bulk hBN microparticles, the exfoliated hBN nanoplatelets improve the mechanical strength of gel electrolytes by 2 orders of magnitude without compromising ionic conductivity. In particular, with shear storage moduli as high as 5 MPa and high room-temperature ionic conductivities in excess of 1 mS cm^{-1}, the exfoliated hBN gel electrolytes provide superlative performance in rechargeable lithium-ion batteries while concurrently suppressing lithium dendrite growth. In addition, the hBN nanoplatelets stabilize the ionic liquid in the gel electrolytes, thereby reducing side reactions with electrodes at high potentials. The resulting high electrochemical stability (>5 V *vs* Li/Li^+) also allows the hBN gel electrolytes to be effectively employed in high-voltage lithium-ion batteries. Finally, the high thermal stability of the hBN gel electrolytes enables the fabrication of rechargeable lithium-ion batteries that can be cycled at rates as high as 10C and high temperatures up to 175 °C. Overall, this work establishes exfoliated hBN ionic liquid gels as a high-voltage solid-state electrolyte that improves the safety and operating temperature range of rechargeable lithium-ion batteries.

METHODS

hBN Exfoliation. A dispersion containing bulk hBN microparticles (~1 μm, Sigma-Aldrich), EC (4 cP viscosity grade, Sigma-Aldrich), and ethanol (Sigma-Aldrich) in a 10:1:52 weight ratio was shear-mixed for 2 h at 10 230 rpm, using a rotor/stator mixer (L5M-A, Silverson) with a square hole screen. The shear-mixed dispersion was then centrifuged (J26-XPI, Beckman Coulter) at 4000 rpm for 20 min to remove large particles, after which the supernatant was collected and mixed with an aqueous solution of 0.04 g mL^{-1} sodium chloride (Sigma-Aldrich) in a 16:9 weight ratio to flocculate exfoliated hBN nanoplatelets and EC. After centrifuging the flocculated solution at 7600 rpm for 6 min, the sedimented hBN nanoplatelets and EC were rinsed with deionized water to remove residual sodium chloride, dried with an infrared lamp, and ground with a mortar and pestle to yield a powder. The hBN/EC powder was then annealed at 400 °C for 2 h in air to decompose EC, resulting in a thin carbon coating on the exfoliated hBN nanoplatelets. The hBN nanoplatelets were observed using a scanning electron microscope (SU8030, Hitachi) and transmission electron microscope (ARM 300F, JEOL), and their lateral size and thickness were characterized using an atomic force microscope (Asylum Research Cypher, Oxford Instruments).

Preparation of hBN Gel Electrolytes. To prepare Li-IL, 1 M LiTFSI (99.95% trace metal basis, Sigma-Aldrich) was dissolved in EMIM-TFSI ($H_2O \leq 500$ ppm, Sigma-Aldrich) by stirring with a magnetic stir bar on a hot plate at 120 °C for 24 h. To produce gel electrolytes, the hBN nanoplatelets (2 g) and Li-IL (3–4 g, 60–67% of gel electrolytes by weight) were mixed using a mortar and pestle (75 mL agate mortar and pestle set, Cole-Parmer) for 30 min. The electrolytes were used after aging for longer than 12 h. All the electrolyte preparation steps were carried out in an argon-filled glovebox.

Characterization of hBN Gel Electrolytes. To evaluate ionic conductivity, the gel electrolyte was inserted between two stainless steel disks, and its resistance (R) was measured by electrochemical impedance spectroscopy (EIS) using a potentiostat (VSP, BioLogic). EIS was performed over a frequency range of 1 MHz–100 mHz and an amplitude of 10 mV. Ionic conductivity (σ) was calculated based on the following equation:

$$\sigma = \frac{t}{R \times A}$$

where t and A are the thickness and area, respectively, of the electrolyte between the stainless steel disks. Temperature-dependent measurements were executed using an environmental chamber (BTX-475, Espec) for precise temperature control. To characterize the lithium ion transference number (T_{Li}), lithium symmetric cells were polarized at 10 mV, and their Nyquist plots were obtained before and after polarization. T_{Li} was then calculated using the following equation:[46]

$$T_{Li} = \frac{I_S(\Delta V - I_0 R_0)}{I_0(\Delta V - I_S R_S)}$$

where ΔV, I, and R are the applied polarization voltage, current from polarization curves, and charge-transfer resistance from the Nyquist plots. Subscripts 0 and S indicate the initial and steady states, respectively. Electrochemical stability was characterized by LSV using the potentionstat. LSV was performed with a scan rate of 1 mV s^{-1} at room temperature, using stainless steel as the working electrode and lithium as both the reference and counter electrodes. Viscoelastic properties (shear storage and loss moduli) were characterized using a rheometer (MCR 302, Anton Paar) equipped with a 25 mm diameter parallel plate (gap between the rheometer stage and parallel plate: 1 mm) with a strain of 0.1% at 25 °C. Compressive elastic moduli were determined using a dynamic mechanical analyzer (RSA-G2, TA Instruments) equipped with 8 mm diameter compression plates (gap: 0.3 mm). The gel electrolyte was compressed to a strain of 1% at a rate of 0.001 mm s^{-1}, and the elastic modulus was calculated from the slope of the stress–strain curve. Thermal stability was studied using a themogravimetric analyzer (TGA/SDTA851, Mettler Toledo) under a nitrogen atmosphere and temperature ramp rate of 7.5 °C min^{-1}. Galvanostatic polarization tests were conducted using CR2032-type lithium symmetric cells at room temperature.

Electrode Preparation. To prepare LTO, LFP, and LNMO electrodes, a slurry of active materials (LTO from Sigma-Aldrich, LFP and LNMO from MTI Corporation), carbon black (Alfa Aesar), and PVDF (MTI Corporation) in an 8:1:1 weight ratio in 1-methyl-2-pyrrolidinone (NMP, Sigma-Aldrich) was coated on aluminum substrates. The electrodes were used after drying in a vacuum oven at 80 °C for longer than 24 h. NMC electrode sheets were obtained from Sigma-Aldrich and used as received. To prepare Gr-LFP electrodes, a slurry of LFP, graphene, and EC in a 45:5:6 weight ratio in NMP was coated on aluminum substrates. The electrodes were used after annealing at 320 °C for 1 h in argon to remove EC. Active material loading was 2, 2, 3, 5, and 4 mg cm^{-2} for LTO, LFP, Gr-LFP, NMC, and LNMO electrodes, respectively.

Battery Testing. Electrodes were cut into circles with a diameter of 1 cm. To improve the interfacial contact between the electrode and gel electrolyte, a small amount (~10 mg) of Li-IL was drop-cast onto the electrode, and the excess on the electrode surface was removed with a Kimtech wipe. The hBN gel electrolyte (~200 mg) was then manually deposited onto the electrode using a spatula, and a counter electrode was placed on the gel electrolyte. Using the stacked electrodes and electrolyte, CR2032-type coin cells were fabricated for testing at room temperature, and split test cells (MTI Corporation) with polytetrafluoroethylene O-rings and a stainless steel spring were assembled for testing at 175 °C. The thickness of the hBN gel electrolytes for all electrochemical tests was 200–250 μm, which was

DOI: 10.1021/acsnano.9b04989
ACS Nano 2019, 13, 9664–9672

measured after disassembling tested cells. Control cells with the Li-IL electrolyte were prepared using a glass microfiber filter (260 μm thick, GF/C grade, Whatman) as a separator. All battery cells were assembled in an argon-filled glovebox and measured with a battery testing system (BT-2143, Arbin).

ASSOCIATED CONTENT

Supporting Information

The Supporting Information is available free of charge on the ACS Publications website at DOI: 10.1021/acsnano.9b04989.

Photograph, XPS, and size distribution of exfoliated, carbon-coated hBN nanoplatelets; additional TEM images of hBN nanoplatelets with and without carbon coating; EIS of a lithium symmetric cell; optical images of lithium dendrite growth; lithium plating/stripping tests; viscoelastic properties, LSV, and TGA of hBN gel electrolytes; photograph of a Gr-LFP electrode; temperature dependence of ionic conductivity of hBN gel electrolytes; and charge−discharge voltage profiles of Gr-LFP|hBN gel|Li cells at high C-rates at 175 °C (PDF)

AUTHOR INFORMATION

Corresponding Author

*E-mail: m-hersam@northwestern.edu.

ORCID

Mark C. Hersam: 0000-0003-4120-1426

Author Contributions

W.J.H. and M.C.H. designed the experiments. W.J.H. and A.C.M.M. prepared hBN nanoplatelets. W.J.H. formulated gel electrolytes, characterized mechanical and electrochemical properties, and performed SEM and TGA analysis. A.C.M.M. conducted XPS analysis. J.-M.L. conducted TEM analysis. J.R.D. conducted AFM analysis. J.-M.L., J.R.D., K.-Y.P., and M.T.Z.T. prepared battery electrodes. W.J.H. fabricated and tested battery cells. W.J.H. and M.C.H. wrote the manuscript. All authors discussed the results and commented on the manuscript.

Notes

The authors declare no competing financial interest.

ACKNOWLEDGMENTS

The electrolyte development was primarily supported by MilliporeSigma. Electrochemical characterization was supported by the Center for Electrochemical Energy Science, an Energy Frontier Research Center funded by the U.S. Department of Energy (DOE), Office of Science, Basic Energy Sciences, under Award No. DE-AC02-06CH11357. Graphene powder processing was supported by the National Science Foundation Scalable Nanomanufacturing Program (NSF CMMI-1727846). SEM, TEM, and XPS were performed in the NUANCE facility at Northwestern University, which is supported by the Soft and Hybrid Nanotechnology Experimental (SHyNE) Resource (NSF ECCS-1542205), the Materials Research Science and Engineering Center (NSF DMR-1720139), the State of Illinois, and Northwestern University. Rheometry and thermogravimetric analysis were performed in the MatCI facility, which receives support from the NSF MRSEC Program (NSF DMR-1720139).

REFERENCES

(1) Chu, S.; Majumdar, A. Opportunities and Challenges for a Sustainable Energy Future. *Nature* **2012**, *488*, 294−303.

(2) Sun, Y.; Liu, N.; Cui, Y. Promises and Challenges of Nanomaterials for Lithium-Based Rechargeable Batteries. *Nat. Energy* **2016**, *1*, 16071.

(3) Schmuch, R.; Wagner, R.; Hörpel, G.; Placke, T.; Winter, M. Performance and Cost of Materials for Lithium-Based Rechargeable Automotive Batteries. *Nat. Energy* **2018**, *3*, 267−278.

(4) Dunn, B.; Kamath, H.; Tarascon, J.-M. Electrical Energy for the Grid: A Choice of Battery. *Science* **2011**, *334*, 928−935.

(5) Goodenough, J. B.; Park, K.-S. The Li-Ion Rechargeable Battery: A Perspective. *J. Am. Chem. Soc.* **2013**, *135*, 1167−1176.

(6) Tarascon, J.-M.; Armand, M. Issues and Challenges Facing Rechargeable Lithium Batteries. *Nature* **2001**, *414*, 359−367.

(7) Balakrishnan, P. G.; Ramesh, R.; Prem Kumar, T. Safety Mechanisms in Lithium-Ion Batteries. *J. Power Sources* **2006**, *155*, 401−414.

(8) Manthiram, A.; Yu, X.; Wang, S. Lithium Battery Chemistries Enabled by Solid-State Electrolytes. *Nat. Rev. Mater.* **2017**, *2*, 16103.

(9) Gao, Z.; Sun, H.; Fu, L.; Ye, F.; Zhang, Y.; Luo, W.; Huang, Y. Promises, Challenges, and Recent Progress of Inorganic Solid-State Electrolytes for All-Solid-State Lithium Batteries. *Adv. Mater.* **2018**, *30*, 1705702.

(10) Lau, J.; DeBlock, R. H.; Butts, D. M.; Ashby, D. S.; Choi, C. S.; Dunn, B. S. Sulfide Solid Electrolytes for Lithium Battery Applications. *Adv. Energy Mater.* **2018**, *8*, 1800933.

(11) Thangadurai, V.; Narayanan, S.; Pinzaru, D. Garnet-Type Solid-State Fast Li Ion Conductors for Li Batteries: Critical Review. *Chem. Soc. Rev.* **2014**, *43*, 4714−4727.

(12) Bideau, J. L.; Viaub, L.; Vioux, A. Ionogels, Ionic Liquid Based Hybrid Materials. *Chem. Soc. Rev.* **2011**, *40*, 907−925.

(13) Chen, N.; Zhang, H.; Li, L.; Chen, R.; Guo, S. Ionogel Electrolytes for High-Performance Lithium Batteries: A Review. *Adv. Energy Mater.* **2018**, *8*, 1702675.

(14) Lewandowski, A.; Świderska-Mocek, A. Ionic Liquids as Electrolytes for Li-Ion Batteries-An Overview of Electrochemical Studies. *J. Power Sources* **2009**, *194*, 601−609.

(15) Garcia, B.; Lavallée, S.; Perron, G.; Michot, C.; Armand, M. Room Temperature Molten Salts as Lithium Battery Electrolyte. *Electrochim. Acta* **2004**, *49*, 4583−4588.

(16) Kim, G. T.; Jeong, S. S.; Xue, M. Z.; Balducci, A.; Winter, M.; Passerini, S.; Alessandrini, F.; Appetecchi, G. B. Development of Ionic Liquid-Based Lithium Battery Prototypes. *J. Power Sources* **2012**, *199*, 239−246.

(17) Choudhury, S.; Mangal, R.; Agrawal, A.; Archer, L. A. A Highly Reversible Room-Temperature Lithium Metal Battery Based on Crosslinked Hairy Nanoparticles. *Nat. Commun.* **2015**, *6*, 10101.

(18) Stone, G. M.; Mullin, S. A.; Teran, A. A.; Hallinan, D. T.; Minor, A. M.; Hexemer, A.; Balsara, N. P. Resolution of the Modulus *versus* Adhesion Dilemma in Solid Polymer Electrolytes for Rechargeable Lithium Metal Batteries. *J. Electrochem. Soc.* **2012**, *159*, A222.

(19) Lu, Y.; Korf, K.; Kambe, Y.; Tu, Z.; Archer, L. A. Ionic-Liquid-Nanoparticle Hybrid Electrolytes: Applications in Lithium Metal Batteries. *Angew. Chem., Int. Ed.* **2014**, *53*, 488−492.

(20) Patel, M.; Gnanavel, M.; Bhattacharyya, A. J. Utilizing an Ionic Liquid for Synthesizing a Soft Matter Polymer "Gel" Electrolyte for High Rate Capability Lithium-Ion Batteries. *J. Mater. Chem.* **2011**, *21*, 17419−17424.

(21) Lu, Y.; Moganty, S. S.; Schaefer, J. L.; Archer, L. A. Ionic Liquid-Nanoparticle Hybrid Electrolytes. *J. Mater. Chem.* **2012**, *22*, 4066−4072.

(22) Moganty, S. S.; Jayaprakash, N.; Nugent, J. L.; Shen, J.; Archer, L. A. Ionic-Liquid-Tethered Nanoparticles: Hybrid Electrolytes. *Angew. Chem., Int. Ed.* **2010**, *49*, 9158−9161.

(23) Lee, J. H.; Lee, A. S.; Hong, S. M.; Hwang, S. S.; Koo, C. M. Hybrid Ionogels Derived from Polycationic Polysilsesquioxanes for Lithium Ion Batteries. *Polymer* **2017**, *117*, 160−166.

DOI: 10.1021/acsnano.9b04989
ACS Nano 2019, 13, 9664−9672

(24) Pablos, J. L.; Garcia, N.; Garrido, L.; Guzman, J.; Catalina, F.; Corrales, T.; Tiemblo, P. Highly Efficient Mixed Li^+ Transport in Ion Gel Polycationic Electrolytes. *J. Membr. Sci.* **2018**, *545*, 133−139.
(25) Lee, J. H.; Lee, A. S.; Lee, J.-C.; Hong, S. M.; Hwang, S. S.; Koo, C. M. Hybrid Ionogel Electrolytes for High Temperature Lithium Batteries. *J. Mater. Chem. A* **2015**, *3*, 2226−2233.
(26) Kubota, Y.; Watanabe, K.; Tsuda, O.; Taniguchi, T. Deep Ultraviolet Light-Emitting Hexagonal Boron Nitride Synthesized at Atmospheric Pressure. *Science* **2007**, *317*, 932−934.
(27) Kim, K. K.; Hsu, A.; Jia, X.; Kim, S. M.; Shi, Y.; Hofmann, M.; Nezich, D.; Rodriguez-Nieva, J. F.; Dresselhaus, M.; Palacios, T.; Kong, J. Synthesis of Monolayer Hexagonal Boron Nitride on Cu Foil Using Chemical Vapor Deposition. *Nano Lett.* **2012**, *12*, 161−166.
(28) Yan, K.; Lee, H.-W.; Gao, T.; Zheng, G.; Yao, H.; Wang, H.; Lu, Z.; Zhou, Y.; Liang, Z.; Liu, Z.; Chu, S.; Cui, Y. Ultrathin Two-Dimensional Atomic Crystals as Stable Interfacial Layer for Improvement of Lithium Metal Anode. *Nano Lett.* **2014**, *14*, 6016−6022.
(29) Rodrigues, M. F.; Kalaga, K.; Gullapalli, H.; Babu, G.; Reddy, A. L. M.; Ajayan, P. M. Hexagonal Boron Nitride-Based Electrolyte Composite for Li-Ion Battery Operation from Room Temperature to 150 °C. *Adv. Energy Mater.* **2016**, *6*, 1600218.
(30) Liang, Y. T.; Hersam, M. C. Highly Concentrated Graphene Solutions *via* Polymer Enhanced Solvent Exfoliation and Iterative Solvent Exchange. *J. Am. Chem. Soc.* **2010**, *132*, 17661−17663.
(31) Ueno, K.; Imaizumi, S.; Hata, K.; Watanabe, M. Colloidal Interaction in Ionic Liquids: Effects of Ionic Structures and Surface Chemistry on Rheology of Silica Colloidal Dispersions. *Langmuir* **2009**, *25*, 825−831.
(32) Luo, W.; Gong, Y.; Zhu, Y.; Li, Y.; Yao, Y.; Zhang, Y.; Fu, K. K.; Pastel, G.; Lin, C. F.; Mo, Y.; Wachsman, E. D.; Hu, L. Reducing Interfacial Resistance between Garnet-Structured Solid-State Electrolyte and Li-Metal Anode by a Germanium Layer. *Adv. Mater.* **2017**, *29*, 1606042.
(33) Ohta, S.; Kobayashi, T.; Seki, J.; Asaoka, T. Electrochemical Performance of an All-Solid-State Lithium Ion Battery with GarnetType Oxide Electrolyte. *J. Power Sources* **2012**, *202*, 332−335.
(34) Monroe, C.; Newman, J. The Impact of Elastic Deformation on Deposition Kinetics at Lithium/Polymer Interfaces. *J. Electrochem. Soc.* **2005**, *152*, A396−A404.
(35) Rosso, M.; Gobron, T.; Brissot, C.; Chazalviel, J.-N.; Lascaud, S. Onset of Dendritic Growth in Lithium/Polymer Cells. *J. Power Sources* **2001**, *97*−*98*, 804−806.
(36) Liang, Z.; Zheng, G. Y.; Liu, C.; Liu, N.; Li, W. Y.; Yan, K.; Yao, H. B.; Hsu, P. C.; Chu, S.; Cui, Y. Polymer Nanofiber-Guided Uniform Lithium Deposition for Battery Electrodes. *Nano Lett.* **2015**, *15*, 2910−2916.
(37) Matsumoto, H.; Sakaebe, H.; Tatsumi, K. Preparation of Room Temperature Ionic Liquids Based on Aliphatic Onium Cations and Asymmetric Amide Anions and Their Electrochemical Properties as a Lithium Battery Electrolyte. *J. Power Sources* **2005**, *146*, 45−50.
(38) MacNeil, D. D.; Lu, Z.; Chen, Z.; Dahn, J. R. A Comparison of the Electrode/Electrolyte Reaction at Elevated Temperatures for Various Li-Ion Battery Cathodes. *J. Power Sources* **2002**, *108*, 8−14.
(39) Rodrigues, M.-T. F.; Babu, G.; Gullapalli, H.; Kalaga, K.; Sayed, F. N.; Kato, K.; Joyner, J.; Ajayan, P. M. A Materials Perspective on Li-Ion Batteries at Extreme Temperatures. *Nat. Energy* **2017**, *2*, 17108.
(40) Chen, K.-S.; Xu, R.; Luu, N. S.; Secor, E. B.; Hamamoto, K.; Li, Q.; Kim, S.; Sangwan, V. K.; Balla, I.; Guiney, L. M.; Seo, J.-W. T.; Yu, X.; Liu, W.; Wu, J.; Wolverton, C.; Dravid, V. P.; Barnett, S. A.; Lu, J.; Amine, K.; Hersam, M. C. Comprehensive Enhancement of Nanostructured Lithium-Ion Battery Cathode Materials *via* Conformal Graphene Dispersion. *Nano Lett.* **2017**, *17*, 2539−2546.
(41) Hayamizu, K.; Aihara, Y.; Nakagawa, H.; Nukuda, T.; Price, W. S. Ionic Conduction and Ion Diffusion in Binary Room-Temperature Ionic Liquids Composed of [emim][BF_4] and $LiBF_4$. *J. Phys. Chem. B* **2004**, *108*, 19527−19532.
(42) Grandjean, A.; Malki, M.; Simonnet, C.; Manara, D.; Penelon, B. Correlation between Electrical Conductivity, Viscosity, and Structure in Borosilicate Glass-Forming Melts. *Phys. Rev. B: Condens. Matter Mater. Phys.* **2007**, *75*, 054112.
(43) Andersson, A. S.; Thomas, J. O.; Kalska, B.; Häggström, L. Thermal Stability of $LiFePO_4$-Based Cathodes. *Electrochem. Solid-State Lett.* **1999**, *3*, 66−68.
(44) Takahashi, M.; Tobishima, S.; Takei, K.; Sakurai, Y. Reaction Behavior of $LiFePO_4$ as a Cathode Material for Rechargeable Lithium Batteries. *Solid State Ionics* **2002**, *148*, 283−289.
(45) Delacourt, C.; Poizot, P.; Tarascon, J.-M.; Masquelier, C. The Existence of a Temperature-Driven Solid Solution in Li_xFePO_4 for $0 \leq x \leq 1$. *Nat. Mater.* **2005**, *4*, 254−260.
(46) Evans, J.; Vincent, C. A.; Bruce, P. G. Electrochemical Measurement of Transference Numbers in Polymer Electrolytes. *Polymer* **1987**, *28*, 2324−2328.

DOI: 10.1021/acsnano.9b04989
ACS Nano 2019, 13, 9664−9672